Data reduction of plasma lines in Incoherent Scatter Radar spectrum

Mini Gupta[1] , Patrick Guio[1,2] and Juha Vierinen[1]
(1) Department of Physics and Technology, UiT The Arctic University of Norway, Tromsø, Norway (mini.gupta@uit.no),
(2) Department of Physics and Astronomy, University College London, London, UK (p.guio@ucl.ac.uk)

This presentation participates in OSPP
Outstanding Student & PhD candidate Presentation contest
Sharing is encouraged

UiT The Arctic University of Norway

Abstract

In the ionosphere, a sustained population of suprathermal electrons is generated due to photoionization or electron precipitation. At resonance, the phase velocity of the electrons matches the Langmuir phase velocity observed by the Incoherent Scatter Radar (ISR). As a result, the scattered power in the plasma line spectrum is enhanced, thus making it possible to detect them. Plasma lines can be used to improve the accuracy of the estimates of electron density and temperature, study features in the electron velocity distribution of the suprathermal electrons and provide an independent method to calculate ionospheric currents. We analyzed the data collected with the EISCAT Tromsø UHF radar on 27 January 2022. We present a novel technique of data reduction to detect plasma lines and extract parameters. We use the method developed by Ivchenko et al. [2017] to determine the times with enhanced plasma lines. For those times, we model the spectrum with a Gaussian function, where the plasma line intensity, frequency and bandwidth correspond to the amplitude, mean and variance, respectively. We observe photoelectron-enhanced plasma lines between 09:28:15–13:28:15 LT. Most of the detected plasma lines are field-aligned, except for 11:38:15–12:49:30 LT, when they are also detected in other directions. The detection of the plasma lines is accompanied by an increase in the electron density estimates from the ion line.

Introduction

1. Incoherent Scatter Radars (ISRs) transmit electromagnetic pulses into the ionosphere, causing electrons to oscillate and re-radiate power isotropically.
2. The scattered signal can be analyzed as a frequency spectrum, providing information about collective plasma interactions.
3. At resonance, large amounts of scattered power at a pair of frequencies, known as ion and plasma lines.
4. Ion lines can be used to estimate ionospheric parameters like density, temperature, and drift velocity.
5. Ratio of the integrated power in the plasma line (I_p) and the ion line (I_i)

$$\frac{I_p}{I_i} \approx (k\lambda_D)^2 \ll 1 \tag{1}$$

where k is the wavenumber and λ_D is the Debye length.
6. Plasma lines can improve estimations of electron density and temperature, and aid in the estimation of ionospheric currents.

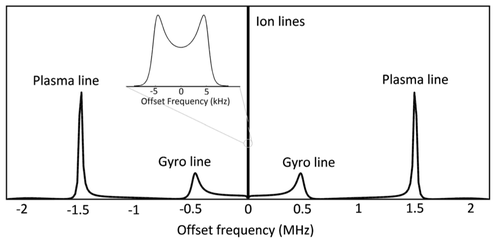

Figure 1: Incoherent Scatter Radar spectrum [Akbari et al., 2017]

Experiment

1. EISCAT Tromsø UHF radar measurements on 27 January 2022
2. BEATA experiment with triangular scan (IP2 mode)
3. Scattering wavenumber of $38.857\,\mathrm{m}^{-1}$. Radar wavelength: $0.324\,\mathrm{m}$.
4. 32-bit alternating code, baud length of $20\,\mu\mathrm{s}$, 64 subcycles per code with a subcycle length $5.58\,\mathrm{ms}$, cycle duration of $0.357\,\mathrm{s}$.
5. Radar scan sequence:

Pointing Direction	Elevation Angle	Azimuth Angle	Dwell time
Field-Aligned (at 240 km)	77.8°	189°	60 s
Vertical	90°	261.1°	30 s
East	75.4°	259.6°	60 s
Vertical	90°	190.5°	30 s

Table 1: Radar scan direction and angles

6. 15 seconds manoeuvre time between pointing directions
7. Plasma line autocorrelation functions (ACFs) recorded with a lag step of $0.4\,\mu\mathrm{s}$
8. Data dumped every $5\,\mathrm{s}$
9. Plasma line data from two downshifted receiver bands (-2.75 to $-5.25\,\mathrm{MHz}$, -5.15 to $-7.65\,\mathrm{MHz}$)

Channel Type	Spectral Resolution	Range Span	Range Resolution
Plasma Line	1.56 kHz	107–374 km	3 km
Ion Line	1.22 kHz	49–693 km	1.5 km

Table 2: Characteristics of Plasma and Ion Line Channels

10. Daytime plasma line analysis from 07:00 LT to 15:00 LT

Method

The EISCAT radars collect raw data as ACF, which is used to estimate the ISR spectrum using the Wiener-Khinchin theorem. An image processing method by Ivchenko et al. [2017] is applied to detect the times and altitudes of the plasma lines (Fig. 2). Ultimately, the spectra are obtained as a function of altitude, frequency and time. Plasma lines are detected $10\,\%$ of the time between 09:28:15–13:28:15 LT.

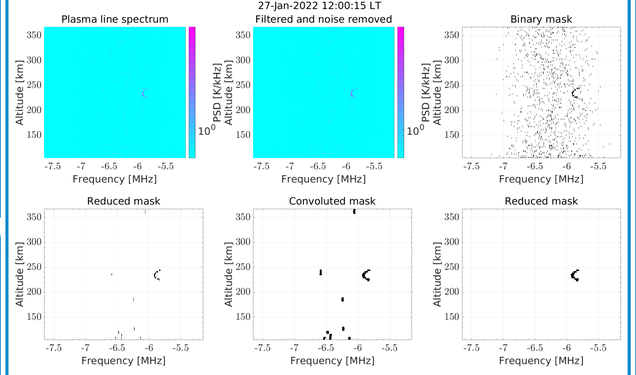

Figure 2: Image morphological processing for plasma line detection

At those specific times and altitudes, the plasma line spectra are fitted to a Gaussian function [Guio et al., 1996] using the Levenberg-Marquardt algorithm, providing estimates for plasma line intensity A_p, frequency f_r and bandwidth δ_f (Fig. 3).

$$S(f; A_p, f_r, \delta_f) = \frac{A_p}{\sqrt{2\pi}\delta_f} \exp\left(-\frac{(f-f_r)^2}{2(\delta_f)^2}\right) \tag{2}$$

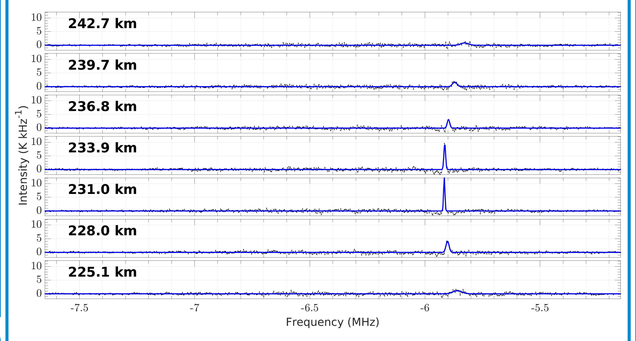

Figure 3: Plasma line spectrum fitted to a Gaussian model

The resulting parameters and their uncertainties are plotted as a function of height in Fig. 4. Uncertainties are quantified by $95\,\%$ confidence intervals around the estimated parameter. The altitude variation of the plasma line frequency corresponds to the electron density variation, and the small uncertainty in the plasma line frequency makes it a precise measure of electron density.

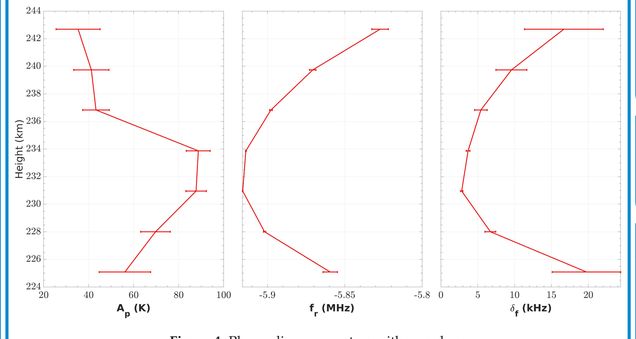

Figure 4: Plasma line parameters with error bars

Acknowledgements

The authors thank Dr Ingemar Häggström for his guidance in analyzing the EISCAT radars plasma line data.

Results

During plasma line detections (marked by black vertical lines in Fig. 5), estimates of electron density and temperature from the ion line analysis show enhancements. The time-altitude variations of the electron density from the ion line follow the time-altitude detections of the plasma lines Fig. 4.

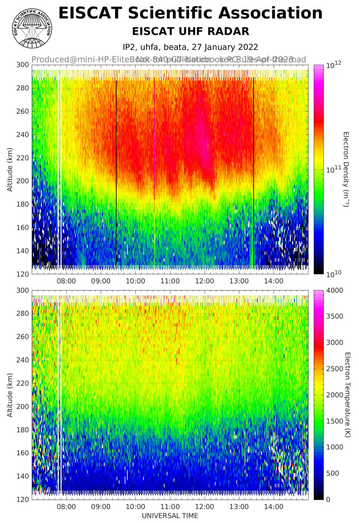

Figure 5: Ionospheric parameters estimated from the ion line analysis

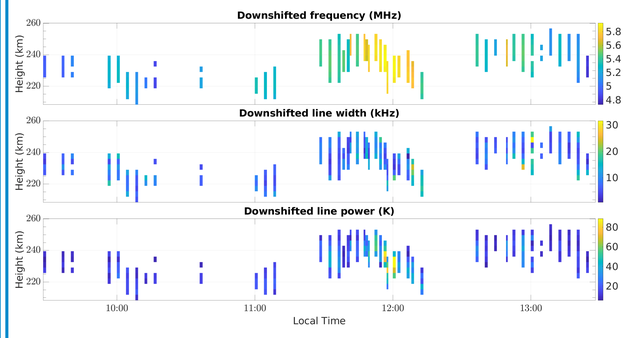

Figure 6: Estimated plasma line parameters over height and time

The plasma line enhancements can be seen at frequencies ranging between 4.73–$5.93\,\mathrm{MHz}$. The plasma line temperature and frequency increase around noon local time (Fig. 6), possibly due to the increasing photoelectron production rate. The variation in the estimated parameters is quite smooth. Fig. 7 displays the average plasma line temperature between three range gates. The plasma line intensity gradually increases with the phase energy of electrons. This result is in accordance with Nilsson et al. [1996] where the plasma line intensity gradually grows from 1.8 to $2.7\,\mathrm{eV}$. Plasma lines at higher altitudes between 2.4–$2.6\,\mathrm{eV}$ of phase energy of electrons show lower intensity than those at lower altitudes. This might be attributed to differences in the photoelectron fluxes at various heights, which could be confirmed through simulations of plasma line intensity as a function of suprathermal electron fluxes at different heights.

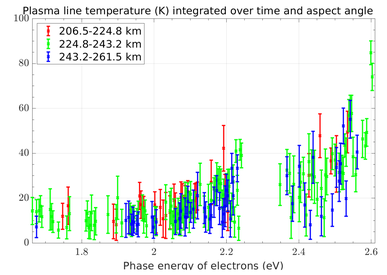

Figure 7: Plasma line intensity integrated over time, aspect angles and height as a function of phase energy of electrons

Fig. 8 shows the variation of the intensity of the plasma line with the aspect angle (i.e. the angle between the radar scattering wavevector and the local magnetic field) and the phase energy of the electrons, with error bars for the intensities. Since electron conductivities are highest along the magnetic field line, radar pointing in the field-aligned direction yields the strongest plasma line temperature. However, enhancements in plasma lines in vertical and east directions are also observed. Guio and Lilensten [1999] conducted a similar study using VHF radar data to investigate the temperature of plasma lines in the tail of the electron velocity distribution, specifically in the range of 24–$28\mathrm{eV}$.

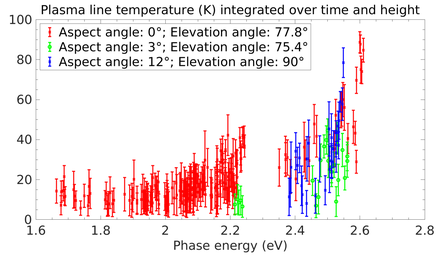

Figure 8: Plasma line intensity integrated over time and height as a function of phase energy of electrons and aspect angles

Conclusion

1. Implemented a method that calculates ISR spectra from ACF and detects plasma lines.
2. Plasma lines detected from 09:28:15 LT to 13:28:15 LT, $10\,\%$ of the time.
3. Different electron energy spectra regions scanned, plasma lines give information on higher energy around noon.
4. Plasma lines were mostly observed in the field-aligned direction, but also observed in other directions from 11:38:15–12:49:30 LT.
5. Plasma lines observed due to Langmuir wave-electron resonance at phase energies of electrons from 1.66–$2.62\,\mathrm{eV}$, with the plasma line intensity gradually increasing in this range.
6. Field-aligned plasma lines have a higher intensity than those at an aspect angle.

Future Work

A model is being developed to estimate the ISR spectrum at angles to the magnetic field, and the presented data will serve to validate it. However, as this work is a proof of concept, additional data is necessary to study the variation of plasma lines with aspect angle. One potential source of additional data for studying the aspect angle variation of plasma lines is EISCAT 3D, which can provide high-time resolution data on plasma lines at angles to the magnetic field.

References

Hassanali Akbari, Asti Bhatt, Cesar La Hoz, and Joshua L. Semeter. Incoherent Scatter Plasma Lines: Observations and Applications. *Space Sci. Rev.*, 212(1-2):249–294, October 2017. doi: 10.1007/s11214-017-0355-7.

P. Guio and J. Lilensten. Effect of suprathermal electrons on the intensity and doppler frequency of electron plasma lines. *Ann. Geophysicæ*, 17:903–912, July 1999. doi: 10.1007/s00585-999-0903-x.

P. Guio, N. Bjørnå, and W. Kofman. Alternating-code experiment for plasma-line studies. *Ann. Geophysicæ*, 14:1473–1479, December 1996. doi: 10.1007/s00585-996-1473-9.

Nickolay Ivchenko, Nicola M. Schlatter, Hanna Dahlgren, Yasunobu Ogawa, Yuka Sato, and Ingemar Häggström. Plasma line observations from the EISCAT Svalbard Radar during the International Polar Year. *Ann. Geophysicæ*, 35(5):1143–1149, October 2017. doi: 10.5194/angeo-35-1143-2017.

H. Nilsson, S. Kirkwood, J. Lilensten, and M. Galand. Enhanced incoherent scatter plasma lines. *Ann. Geophysicæ*, 14(12):1462–1472, December 1996. doi: 10.1007/s00585-996-1462-z.